

ORIGINAL ARTICLE

Chemical interactions between an active pharmaceutical ingredient and its counterion in a tromethamine salt under forced degradation conditions

Eric Loeser¹, Paul Sutton¹, Ada Skorodinsky¹, Melissa Lin², and Guy Yowell¹

¹Pharmaceutical and Analytical Development, Novartis, East Hanover, NJ, USA and ²Chemical and Analytical Development, Novartis, East Hanover, NJ, USA

Abstract

In this study, the tromethamine salt of an active pharmaceutical ingredient containing both a carboxylic acid and ethyl ester functionality was subjected to forced degradation conditions. Based on HPLC-MS analysis, it was found that tromethamine formed both amide and ester type condensation products with the API, with amide formation predominating over ester formation. Addition of tromethamine at the carboxylic acid group of the API was favored over addition at the ethyl ester group. Tromethamine condensation products were observed only under the harshest stress conditions (80 degrees and 75% relative humidity), in which the salt physically changed from a crystalline form to a deliquesced state. Under stress conditions in which the crystalline structure of the salt remained intact, good stability was observed. Thus, the interaction between tromethamine and API occurred only in cases where the crystallinity of the salt was compromised.

Keywords: Preformulation, stability, tris base, tris(hydroxymethyl)aminomethane, 2-Amino-2-hydroxymethylpropane-1,3-diol, salt selection, THAM

Introduction

The conversion of an active pharmaceutical ingredient (API) from its free acid or free base form into a salt form during drug development is a common strategy for improving the properties of the API. An organic amine base which has found use as a cationic salt forming agent in pharmaceutical development is tromethamine^{1,2}. Its status as a class II counterion³ means that it is generally accepted as being non-toxic and innocuous, which is a very important aspect of any drug component intended for human use. Ketorolac tromethamine⁴ is a well known example of a tromethamine salt which has found use in marketed pharmaceutical products.

Studies have shown that in some cases tromethamine salts show improved physical properties to sodium salt forms of APIs which contain a carboxylic acid moiety^{5,6}. However, the possibility of a chemical reaction occurring between tromethamine and its API salt partner has received little attention. We are aware of only one such

report⁶, in which the tromethamine salt of an experimental API was subjected to a variety of stress conditions. It was reported that, at relatively extreme conditions of 80°C, HPLC-MS showed evidence of a degradation product which appeared to be produced by a condensation reaction between tromethamine and the API, presumably forming an amide or ester with the loss of one water molecule. The possibility of either amide or ester formation is due to the presence of a primary amino group and three hydroxy groups within the structure of tromethamine.

Recently, we conducted preformulation studies of a Neutral Endopeptidase Inhibitor (NEP) pro-drug, which contains both a carboxylic acid group and an ethyl ester group in its molecular structure, and which has recently been utilized in a combination drug product under clinical study^{7–10}. The physical properties of several salt forms of the API, including a tromethamine salt, were compared. With regard to hygroscopicity, the tromethamine salt showed a significant improvement relative to the sodium

Address for Correspondence: Eric Loeser, Pharmaceutical and Analytical Development, Novartis, East Hanover, NJ, USA.
E-mail: eric.loeser@novartis.com

(Received 23 March 2011; revised 16 June 2011; accepted 01 July 2011)

salt, in accord with studies of other APIs^{5,6}. However, under stress conditions of 80°C with 75% relative humidity (RH), HPLC indicated the appearance of several degradation products in samples of the tromethamine salt which were absent from other salt forms. Suspecting a tromethamine interaction with the API was responsible for these additional HPLC peaks, we attempted to verify the identity of these degradation products and determine which were the most predominant. The following report is a brief account of this finding, which may be of interest to other research and development chemists in the pharmaceutical industry involved in salt screening studies of new APIs.

Experimental

Apparatus

Differential scanning calorimetry (DSC) analysis was conducted using a DSC Q1000 instrument (TA instruments, New Castle, DE), using a heating rate of 10°C/min to obtain melting point (mp) onset temperatures. Dynamic vapor sorption (DVS) analysis was conducted using a SGA 100 symmetric vapor sorption analyzer (VTI scientific instruments, Hialeah, FL). After equilibration in a dry atmosphere, sample mass was monitored over time as RH level was increased in stepwise fashion, and the sample allowed to equilibrate for 2 h at each humidity level before proceeding to the next step. X-ray powder diffraction (XRPD) analysis was conducted using a Bruker D8 Discover X-ray diffractometer (Bruker AXS, Madison, WI) for 2 theta range of 3 to 40 degrees (CuK α , 40 kV, 40 mA).

Structural confirmation of the degradation products was obtained using an HPLC-MS instrumentation consisting of Agilent 1100 HPLC system (Agilent Technologies, Santa Clara, CA), equipped with a Micromass Quattro Micro API detector (Waters, Milford, MA) and a Symmetry C18 column of dimensions 3 × 150 mm, 3.5 μ m (Waters) maintained at 40 degrees. Flow rate was 0.5 mL/min. Mobile phase contained 0.1% formic acid with a gradient of 10–90% acetonitrile (MeCN) over 14 min. Simultaneous MS and UV detection was obtained by routing the HPLC column outlet through the UV and MS detectors in serial fashion.

The forced degradation study was conducted by storing samples in an 80°C oven. To simulate dry storage

conditions, samples in sealed containers were stored into the oven. To test the effect of elevated temperature and humidity (80°C/75% RH conditions), open sample containers were placed into a 75% RH humidity chamber (containing saturated NaCl) which was located inside the same oven.

Preparation of salts

All chemicals were reagent grade (>98% purity) or better. The API was supplied by Novartis (Chemical and Analytical Development, East Hanover, NJ) in the form of the sodium salt, which was crystalline by XRPD and polarizing light microscopy. The tromethamine salt was prepared by first converting the sodium salt to free acid *in situ* (by partitioning between aqueous HCl and ethyl acetate), then adding 1 equivalent of tromethamine and crystallizing the tromethamine salt from the ethyl acetate solution as a white solid, crystalline by XRPD and polarizing light microscopy. The calcium salt was prepared by dissolving sodium salt in water and adding 0.5 equivalent of CaCl₂ to precipitate the hemicalcium salt¹¹. After filtration and drying, the calcium salt was amorphous by XRPD.

All three salts (sodium, calcium, and tromethamine) showed satisfactory elemental analysis (Robertson Microlit Laboratories, Madison, NJ). In addition to the three salts, crystalline free acid form of the API was also prepared, by partitioning the API sodium salt between aqueous HCl and ethyl acetate and removing solvent from the dried ethyl acetate solution using a rotary evaporator. The resulting oil was then dissolved in toluene and evaporated several times at 50°C to remove traces of water, followed by drying under vacuum. The material initially formed a foam which gradually collapsed into a colorless oil. Over several days under vacuum it eventually solidified into a white solid, crystalline by XRPD and polarizing light microscopy.

Results and discussion

Physical properties of the API salts

During preformulation studies of the API, it was found that the free acid form exhibited undesirable physical properties. Previous reports indicated it was isolated as a foam, assumed to be amorphous with no reported melting point⁷. Although a crystalline solid was eventually

Table 1. Mp onsets determined by DSC, weight gain due to water adsorption during DVS analysis at 25°C, and % degradation (HPLC) and changes in physical form based on XRPD pattern after specified stress conditions of 1 week. DVS analysis and stability testing was not conducted for the free acid form. Mp value in parenthesis is literature value⁷.

API Form	mp onset, DSC (°C)	% Water uptake (DVS)			Stability %	
		45% RH	75% RH	85% RH	degradation (HPLC)	crystallinity (XRPD)
free acid	68	–	–	–	–	–
Tromethamine salt	120	0.1	0.3	1.4	0.1 crystalline	26.0 deliquesced
Sodium salt	165 (159–160)	0.3	25.8	36.8	0.1 crystalline	3.2 deliquesced
Hemicalcium salt	>200*	1.9	6.9	13.3	0.2 amorphous	0.4 weak XRPD pattern

*Decomposed upon melting.

obtained in our own laboratory after a laborious isolation procedure, the method of isolation was not amenable to scale up, and the melting point ($<70^{\circ}\text{C}$) was considered too low to allow development into an oral dosage form. For this reason, a salt screen was conducted. In addition to a sodium salt⁷ and a hemicalcium salt⁸, a crystalline tromethamine salt of the API was also identified.

Several physical properties of the various forms are shown in Table 1. The calcium salt was thermally stable to above 200°C but was amorphous. The melting point of the tromethamine salt was substantially higher relative to free acid. The hygroscopicity of the salts was also evaluated. This revealed a very large difference between the tromethamine and other salts. With regard to hygroscopicity, the tromethamine salt showed very low water uptake at RH values as high as 85% compared to the other two salts, making the tromethamine salt the best candidate from a hygroscopicity perspective. This trend toward

significantly lower hygroscopicity of the tromethamine salt relative to the sodium salt appears to be a common phenomenon, having been observed by others for several other carboxylic acid type APIs^{5,6}.

Under dry conditions for one week at 80°C , all three salts remained physically stable, showing no change in crystalline form by XRPD analysis. However, under the more harsh condition of $80^{\circ}\text{C}/75\% \text{ RH}$, the sodium and tromethamine salts were observed to change in physical form from a crystalline solid to a paste-like non-crystalline material. The calcium salt, on the other hand, remained as a free flowing powder and exhibited a weak XRPD pattern, suggesting partial conversion to a hydrate form. With regard to chemical stability, the relative amounts of degradation were closely related to the physical stability. All three salts under dry conditions showed good stability, but the tromethamine and sodium salts which had deliquesced under 75% RH

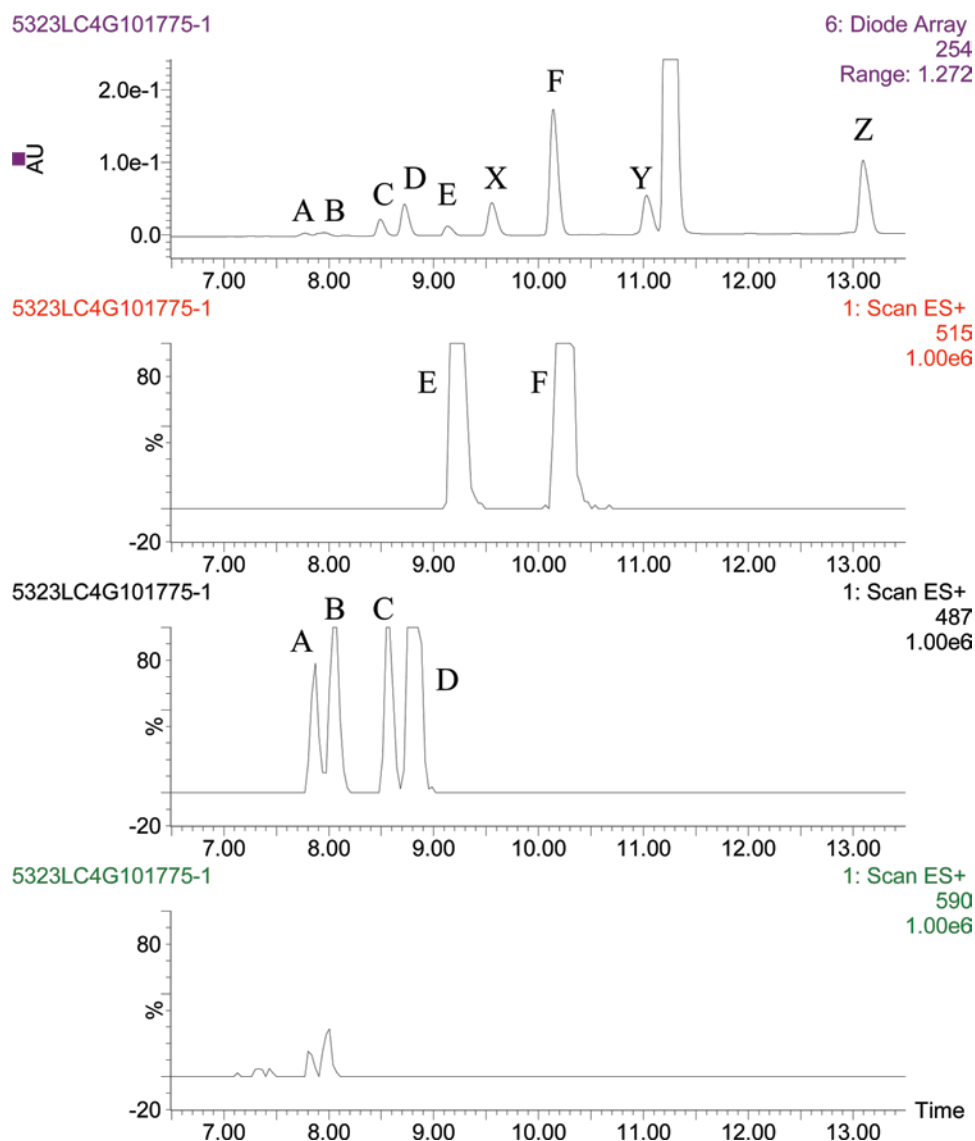


Figure 1. HPLC analysis of tromethamine salt sample after $80^{\circ}\text{C}/75\% \text{ RH}$ conditions. Top chromatographic trace shows UV 254 nm results. Other traces show single ion chromatograms (ES⁺ ionization) from the same sample injection, at m/z 515, 487, and 590, with the extracted m/z value shown at the upper right of each chromatogram. Large peak at 11.3 min is the API.

conditions showed substantial degradation by HPLC (Table 1).

Identification of API-tromethamine condensation products

Based on further analysis by HPLC-MS (Figure 1), several degradation products were identified in the samples

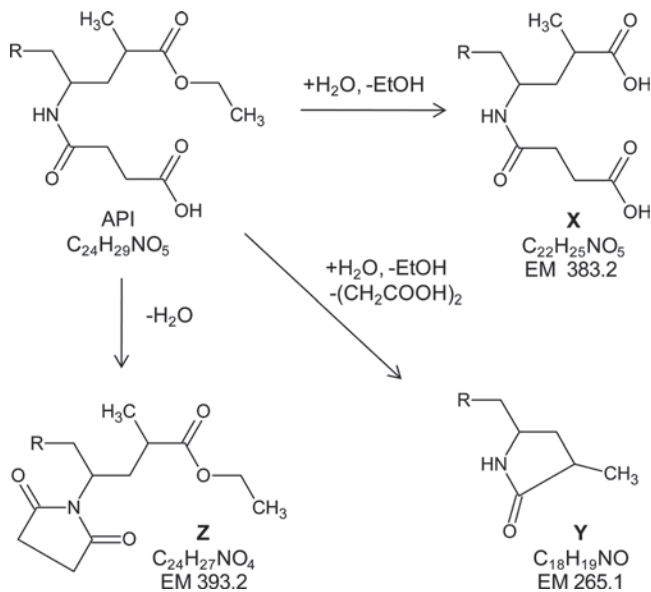


Figure 2. Proposed structures for degradation products which occur in all three salts, for HPLC peaks X, Y, and Z in fig 1, and the corresponding exact mass (EM) values (R group = biphenyl). For simplicity, configuration of the chiral centers is not shown. Observed *m/z* values were 384 and 348 (MH⁺, [MH-EtOH]⁺) for peak X, 531, 307, and 266 ([2M+H]⁺, [MH+MeCN]⁺, MH⁺) for peak Y, 406 and 384 (MNa⁺, MH⁺) for peak Z.

subjected to the most harsh stress condition (80°C/75% RH). Three degradation products (HPLC peaks X-Z) were present in samples of all three salts. Structures of these degradation products was supported by HPLC-MS data and could be rationalized by obvious degradation pathways (Figure 2), such as hydrolysis to a known di-acid structure (peak X, 2.6 area % by UV 254nm) which is the active metabolite of the API^{7,10}, as well as two intramolecular cyclization reactions (peaks Y and Z, 3.0 and 6.5%, respectively). However, several additional peaks appeared in the sample of tromethamine salt which were not present in other salts (peaks A-F, Figure 1). The observed *m/z* values of these additional peaks suggested addition of tromethamine and loss of water for peaks A and B, while peaks C-F were the net result of addition of tromethamine and loss of ethanol. The most reasonable explanation is the occurrence of condensation reactions leading to the expected structures as shown in Figure 3. Addition of tromethamine to the acid group of the API and loss of water results in amide I or ester II. Tromethamine displacing ethanol from the ester group of the API leads to amide III or ester IV. Also, structures I and II after hydrolysis of the ethyl ester group lead to amide V and ester VI, which are constitutional isomers of III and IV.

As an aid to correctly assigning the structures I-VI with HPLC peaks A-F, single ion chromatograms were extracted as shown in Figure 1. Peaks E and F, showing *m/z* 515, correspond to structures I and II, while peaks A and D (*m/z* 487) correspond to structures III-VI. Also included is a single ion chromatogram extracted at *m/z* 590, which is the expected MH⁺ value for two tromethamine molecules adding to a single API molecule with loss of both

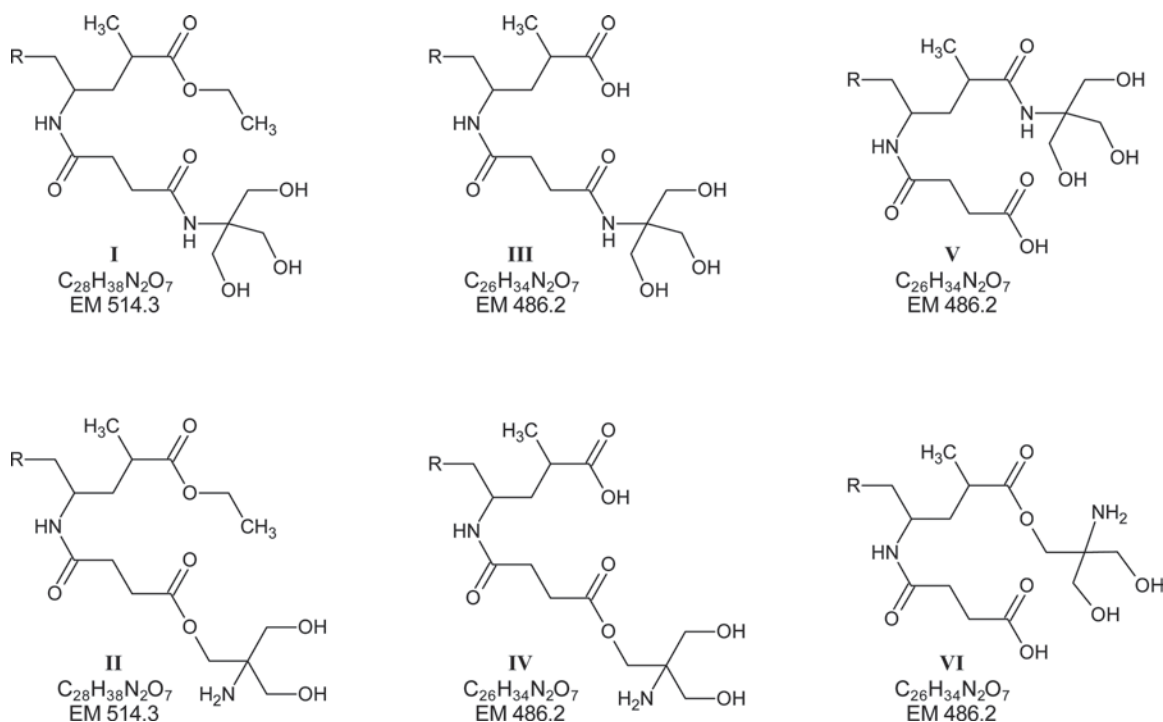


Figure 3. Possible API-tromethamine condensation products.

water and ethanol. Four 2:1 tromethamine/API structures appear to be present at trace level, and two of these peaks are partly coeluting with peaks **A** and **B**. However, we emphasize that the amounts of the 2:1 species are very low, as illustrated by the low intensity of the peaks extracted at m/z 590 compared to the other m/z values, which have all been adjusted to the same intensity scale in Figure 1.

Since the UV absorbance at the detection wavelength (254 nm) is caused by the same chromophore (biphenyl group) which is present in the API and all the degradation product structures it follows that the UV 254 nm chromatogram gives an accurate representation of the relative amounts of each species on a molar basis. Peak **F** is assigned to structure **I**. This assignment is based on three observations. First, it is assumed that the amino nitrogen is more reactive than hydroxyl oxygens of the tromethamine towards condensation with the carboxylic acid group of the API¹². Although one could argue that salt formation creates a barrier to the reaction between a protonated amino group with a carboxylate anion^{13,14},

it is known that, under sufficiently high temperature and when in a melted state, amines and carboxylic acids will react and form the corresponding amides in good yield¹⁵. This reaction gives high yields of amide product even for acid substrates which contain a hydroxyl group¹⁶. Thus, we expect formation of structure **I** is favored over structure **II** and thus peak **F** (9.2% peak area) is assigned to structure **I**, and peak **E** (0.7%) to structure **II**. A second aspect of the data supporting the assignment of structure **I** to peak **F** are differences in the mass spectra obtained from peaks **E** and **F** (Figure 4). The mass spectrum of peak **E**, in addition to showing the MNa^+ adduct (m/z 537), also shows an intense fragment (m/z 497) corresponding to loss of water, in contrast to the spectrum of peak **F** which shows no such fragment. It is reasonable that structure **II**, because it contains a strongly basic amino group, will preferentially form a stable alkylammonium cation in the gas phase within the MS detector, and its mass spectrum will exhibit a dominant molecular ion peak with minimal fragmentation. Structure **I**, on the other hand, does not contain this strongly basic amino

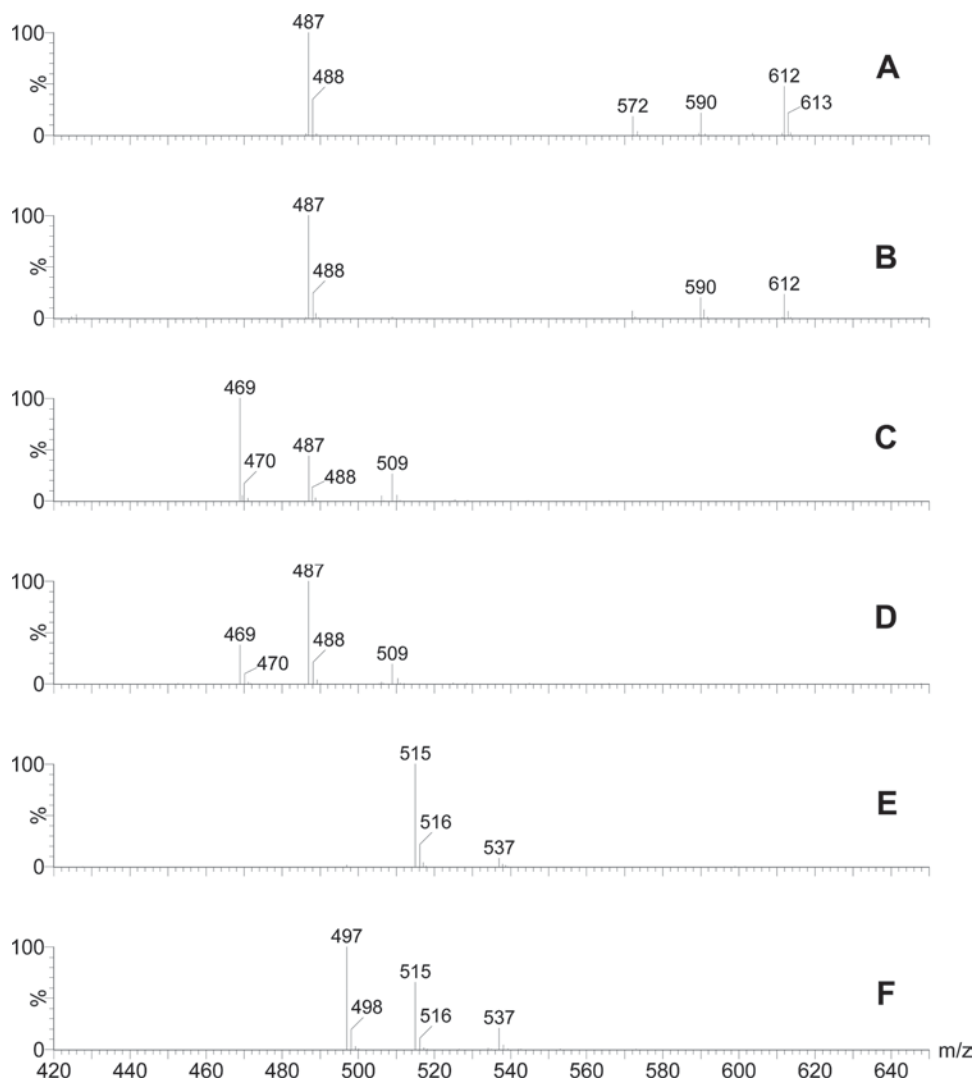


Figure 4. Mass spectra obtained for peaks **A-F**. Peaks **A** and **B**, in addition to major **A** or **B** component MH^+ (m/z 487), also show m/z values of 612, 590, and 572 due to presence of coeluting 2:1 tromethamine-API structures (corresponding to MNa^+ , MH^+ , and $[MH-H_2O]^+$).

nitrogen and thus behaves differently. It is known that, under conditions which favor dehydration, a 1:1 mixture of tromethamine with a carboxylic acid will undergo two successive dehydrations, the first dehydration leading to an amide analogous to structure **I**, and the second dehydration leading to an oxazoline^{17–19}. The general form of such a reaction is shown in Figure 5, which can presumably occur for the protonated amide **I** in the gas phase of the MS detector but not for ester **II**. Thus, the tendency for the mass spectrum of peak **F** to exhibit this very stable $[\text{MH}-\text{H}_2\text{O}]^+$ fragment suggests structure **I**. Finally, a third observation which suggests that peak **F** corresponds to structure **I** is the greater HPLC retention of peak **F** relative to peak **E**. The differences in molecular structure between **I** and **II** are the presence of an amide group in **I** versus an ester group in **II**, and the presence of a hydroxyl group in **I** versus an amino group in **II**. We expect that the positive charge of the protonated amino group of structure **II** under the acidic HPLC mobile phase conditions will be the dominant factor influencing retention of **I** relative to **II**, and cause **I** to elute after **II** based on known trends in reversed phase HPLC retention of model compounds in acidic mobile phases²⁰.

With regard to structural assignment of peaks **A–D**, the HPLC-MS evidence suggests peaks **C** and **D** are amides **III** and **V**, while peaks **A** and **B** are esters **IV** and **VI**. This is based on the same arguments made previously with regard to relative amounts, relative HPLC retention, and mass spectral features. Peaks **C** (1.1%) and **D** (2.2%) are substantially larger than peaks **A** (0.2%) and **B** (0.4%), peaks **C** and **D** elute substantially later than peaks **A** and **B**, and the mass spectra of peaks **C** and **D** show a strong $[\text{MH}-\text{H}_2\text{O}]^+$ fragment (m/z 469) which is absent in spectra of peaks **A** and **B**. However, which amide structure (**III** or **V**) corresponds to which amide peak (**C** or **D**), or which ester structure (**IV** or **VI**) corresponds to which ester peak (**A** or **B**) cannot be assigned for certain without application of more sophisticated structural elucidation tools than the ones used in this study.

Important aspects of API-tromethamine interactions

It is important to note that under dry stress conditions of 80°C, the tromethamine salt was stable, in sharp contrast to the sample stored 1 week under 80°C/75% RH conditions which showed 26% impurities by HPLC-UV. The fact that interactions occur between the API and tromethamine under conditions of 80°C/75% RH, but not

under dry conditions, is counterintuitive when considering that the loss of water is an important aspect of the proposed condensation reactions, and removal of water (or ethanol) should in principle drive the reaction in favor of the condensation products. Accordingly, one would expect that the tromethamine salt samples stored under 75% RH conditions would produce less condensation products than the samples stored under dry condition by impeding the removal of water. The observed opposite behavior suggests that rigorous removal of water is less important than the requirement that the tromethamine salt is in a physically melted state. This is supported by studies on the general reaction of amines and carboxylic acids performed by simple heating of the two compounds without solvent¹⁵. These investigators observed that good yields of amides could be obtained by heating amine and carboxylic acid mixtures at 180°C, provided that the compounds had melting points below the reaction temperature. For compounds which did not melt, the reaction yield was drastically reduced, despite the high temperature employed. This finding can be interpreted as the crystallinity of the reaction components acting as a prohibitive factor against reactivity. In the case of the tromethamine salt, it appears that the presence of humidity is essential for causing the salt to melt or deliquesce into a non-crystalline liquid-like state at 80°C, which is a substantially lower temperature than the normal melting point under dry conditions (Table 1). This loss of crystallinity presumably allows the condensation reactions to proceed to a significant degree, despite the presence of some water in the system. Thus, the physical loss of crystallinity appears to be a key factor in the conversion of tromethamine salt into the observed degradation products. Such a relationship between crystallinity and solid state chemical stability is not uncommon, and an account of this phenomenon has been described in a recent report of early drug development activities for a dual neurokinin receptor antagonist drug²¹.

With regard to the relative amounts of tromethamine addition products in the current study, there is a very clear trend towards tromethamine amide formation versus ester formation. Thus, the observed trends are **I** > **II**, and **III,V** > **IV,VI**. However, another important reactivity aspect is which site within the API structure, the carboxylic acid group or the ethyl ester group, is more prone to addition of tromethamine. The relative amounts of structure **I** and structure **III** reflect the relative reactivity of carboxylic

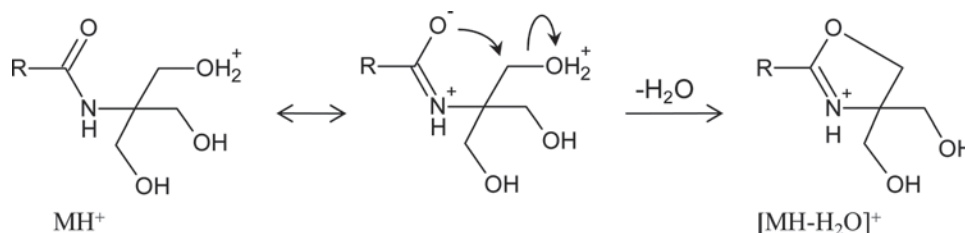


Figure 5. Proposed mechanism for the formation of observed $[\text{MH}-\text{H}_2\text{O}]^+$ fragment in HPLC-MS peaks **A**, **C**, and **D**, due to facile oxazoline formation in tromethamine amide structures **I**, **III**, and **V**.

acid versus ethyl ester groups of the API. These data show a greater tendency for tromethamine to react with the acid group of the API relative to the ethyl ester group. This is based on the observed amount of structure **I** (peak **F**) relative to structure **III** (peak **C** or **D**). Regardless of whether peak **C** or **D** corresponds to structure **III**, the amount of amide **I** formed by addition at the acid group is at least four times higher than amide **III** formed by addition at the ethyl ester group. Based on known relative reactivity of esters versus acids toward substitution²², the observed trend of **I** > **III** is counterintuitive, but is in agreement with a study on the thermally induced reaction of amines with carboxylic acids in solvent-free conditions, where it was reported that esters were substantially less reactive than acids¹⁵. Thus, the greater reactivity of the carboxylic acid group relative to the ester group may be related to the salt forming action between the API and tromethamine, which keeps the amino group and carboxylic acid group in close proximity to each other. However, we recognize that the carboxylic acid and ethyl ester groups of the API are subjected to different intramolecular steric, inductive, and conformational influences. While both the acid and ethyl ester groups can be considered butanoic acid analogues, the number and chemical nature of substituents attached to the butanoic acid chain are different between the carboxylic acid and ethyl ester groups. Consequently, it is difficult to generalize these findings of relative acid versus ethyl ester reactivity towards other APIs which may also contain both an acid and ester group.

Conclusion

This study shows that amide or ester condensation products can be formed from tromethamine salts of carboxylic acid containing APIs under certain forced degradation conditions. It was found that the amino group of tromethamine was significantly more reactive than the hydroxyl groups, resulting in higher levels of tromethamine amide products versus the corresponding tromethamine ester products. Also, it was observed that tromethamine added at both the carboxylic acid group and ethyl ester group of the API, with the carboxylic acid group being favored. However, as observed in a previous study for a different API⁶, it appears that the general reaction between the API and tromethamine is unfavorable and unlikely to occur in samples of crystalline solids which retain their crystalline integrity under the stress conditions. Nevertheless, in our opinion it is prudent to be aware of this potential reaction when new tromethamine salts of APIs are being developed, and a suitable forced degradation exercise using conditions similar to the ones employed in this study will help ensure that any significant condensation product is well separated from other peaks of interest during HPLC method development. This may become important in the event that trace amounts of the impurity begins to appear during stability studies of longer duration than the relatively short studies used during preformulation development.

Also, although the major focus of this report was chemical interactions between tromethamine and the API, it is noteworthy that the tromethamine salt showed substantially lower hygroscopicity relative to the sodium salt, a trend which has been reported for several other APIs^{5,6} and may be of significant practical value.

Acknowledgments

We thank Peter Karpinski of Novartis for helpful discussions.

Declaration of interest

The authors report no conflicts of interest.

References

1. Paulekuhn GS, Dressman JB, Saal C. (2007). Trends in active pharmaceutical ingredient salt selection based on analysis of the Orange Book database. *J Med Chem*, 50:6665–6672.
2. O'Connor KM, Corrigan OI. (2001). Preparation and characterisation of a range of diclofenac salts. *Int J Pharm*, 226:163–179.
3. Stahl PH, Wermuth CG, eds. (2002). *Handbook of Pharmaceutical Salts: Properties, Selection, and Use*. Weinheim: Wiley-VCH, 345.
4. Gupta AK, Madan S, Majumdar DK, Maitra A. (2000). Ketorolac entrapped in polymeric micelles: preparation, characterisation and ocular anti-inflammatory studies. *Int J Pharm*, 209:1–14.
5. Gu L, Strickley RG. (1987). Preformulation salt selection. Physical property comparisons of the tris(hydroxymethyl)aminomethane (THAM) salts of four analgesic/antiinflammatory agents with the sodium salts and the free acids. *Pharm Res*, 4:255–257.
6. Wu Y, Hwang TL, Algayer K, Xu W, Wang H, Procopio A et al. (2003). Identification of oxidative degradates of the TRIS salt of a 5,6,7,8-tetrahydro-1,8-naphthyridine derivative by LC/MS/MS and NMR spectroscopy-interactions between the active pharmaceutical ingredient and its counterion. *J Pharm Biomed Anal*, 33:999–1015.
7. Ksander GM, Ghai RD, deJesus R, Diefenbacher CG, Yuan A, Berry C et al. (1995). Dicarboxylic acid dipeptide neutral endopeptidase inhibitors. *J Med Chem*, 38:1689–1700.
8. Feng L, Godtfredsen SE, Karpinski P, Sutton PA, Prashad M, Girgis MJ, Hu B, Liu Y. (2007). Pharmaceutical combinations of an angiotensin receptor antagonist and an NEP inhibitor. PCT International Application Publication, WO 2007/056546 A1.
9. Kurtz TW, Klein U. (2009). Next generation multifunctional angiotensin receptor blockers. *Hypertens Res*, 32:826–834.
10. Gu J, Noe A, Chandra P, Al-Fayoumi S, Ligueros-Saylan M, Sarangapani R et al. (2010). Pharmacokinetics and pharmacodynamics of LCZ696, a novel dual-acting angiotensin receptor-neprilysin inhibitor (ARNi). *J Clin Pharmacol*, 50: 401–414.
11. Hook D, Wietfeld B, Lotz M. (2009). Process for preparing biaryl substituted 4-amino-butyric acid or derivatives thereof and their use in the production of NEP inhibitors, US Patent Application Publication, US20090326066.
12. Brown WH, Foote CS, Iverson BL, Anslyn EV. (2009). *Organic Chemistry*. Belmont, CA: Brooks/Cole, 338.
13. Vollhardt KPC, Schore NE. (2003). *Organic Chemistry. Structure and Function*, 4th ed. New York: W.H. Freeman, 835.
14. Al-Zoubi RM, Marion O, Hall DG. (2008). Direct and waste-free amidations and cycloadditions by organocatalytic activation of carboxylic acids at room temperature. *Angew Chem Int Ed Engl*, 47:2876–2879.
15. Jursic BS, Zdravkovski Z. (1993). A simple preparation of amides from acids and amines by heating of their mixture. *Synth Commun*, 23, 2761–2770.

16. Gooßen J, Ohlmann DM, Lange PP. (2009). The thermal amidation of carboxylic acids revisited. *Synthesis*, 2009, 160–164.
17. DeJarlais WJ, Gast LE, Cowan JC. (1966). Water-solubilizable oxazoline polyester coating resins. *J Am Oil Chem Soc*, 43, 41–45.
18. Purcell RF. (1967). Nitrocellulose coating composition plasticized with oxazolines. US Patent 3336145.
19. Williams J, Pandarinathan L, Wood J, Vouros P, Makriyannis A. (2006). Endocannabinoid metabolomics: a novel liquid chromatography-mass spectrometry reagent for fatty acid analysis. *AAPS J*, 8:E655–E660.
20. Herre S, Pragst F. (1997). Shift of the high-performance liquid chromatographic retention times of metabolites in relation to the original drug on an RP8 column with acidic mobile phase. *J Chromatogr B Biomed Sci Appl*, 692:111–126.
21. Sigfridsson K, Ahlqvist M, Carlsson A, Fridström A. (2011). Early development evaluation of AZD8081: a substrate for the NK receptors. *Drug Dev Ind Pharm*, 37:702–713.
22. Fox MA, Whitesell JK. (2004). *Organic Chemistry*, 3rd ed. Sudbury, MA: Jones and Bartlett, 600.